

UN
82
S243:
2002

**INCLUSION CHEMISTRY OF
NEUTRAL NONLINEAR OPTICAL DYES
WITHIN ORGANICALLY MODIFIED SILICATES**

By

Ian Saratovsky

**Submitted in partial fulfillment
of the requirements for
Honors in the Department of Chemistry**

UNION COLLEGE

June, 2002

ABSTRACT

SARATOVSKY, IAN Inclusion chemistry of neutral nonlinear optical dyes within organically modified silicates. Department of Chemistry, June 2002.

The field of photonics involves the use of light to acquire, store, process, and transmit information. Nonlinear optical (NLO) materials are crucial for success in the advancement of photonic devices. Laponite and hectorite host assemblies have been shown previously by our group to induce J-aggregation of nonlinear optical (NLO) dyes and offer facile routes to film fabrication. Head-to-tail alignment (J-aggregation) of the NLO chromophores is a required condition for photonic applications. In this study, tetrabutylammonium, triethylhexylammonium, trimethyldodecylammonium, and trimethylcetylammmonium surfactants were utilized to render the smectic intergallery region organophilic thus facilitating chromophore intercalation and an increased J-aggregated dye fraction. Fourier transform infrared spectroscopy and powder X-ray diffraction were used to probe the interlayer structure and phase state of the intercalated alkylammonium surfactants by monitoring frequency shifts of the CH₂ stretching vibrations and gallery height as a function of packing density and chain length. As the chain length or interlayer packing density increased, the chains adopted a more ordered, lamellar structure leading to two-dimensional ordering of clay tactoids. Organically modified laponite was subsequently loaded with two NLO chromophores, disperse red 1 (DSR1) and disperse orange 3 (DSO3), and the effects of surfactants on the extent of J-aggregation were studied. The nature of dye aggregation was characterized using UV/VIS spectroscopy. We report herein that modifying laponite tactoids with surfactants allows for selective control over nonlinear optical chromophore aggregation. In addition, the presence of surfactant within the host framework affords the possibility of higher dye loadings of DSO3 and DSR1 as well as inducing a higher fraction of J-aggregates of DSR1 than previously reported.

ACKNOWLEDGEMENTS

Thank you Mark for showing me the ropes and teaching me that research is a venue for exploration and intellectual amusement. Thank you Amy for spending countless hours synthesizing and characterizing materials, allowing for fundamental understanding of this perplexing, albeit fascinating material. Thank you Mike for being an amazingly interactive mentor, good friend, and for opening my eyes to the world of chemistry. I would also like to thank the Union College Chemistry Department for their endless guidance and advice.

I would like to thank the Union College Surdna summer research fellowship and the Camille and Henry Dreyfus Foundation for financial support. Lastly I would like to thank my family, for without their support and devotion I would not have been able to accomplish so much.

TABLE OF CONTENTS

ABSTRACT	ii
ACKNOWLEDGEMENTS	iii
TABLE OF CONTENTS	iv
TABLE OF FIGURES	v
Introduction	1
Experimental	9
Results and Discussion	12
Conclusions	23
Future Work	24
References	25

TABLE OF FIGURES

Figure 1. Structure of TOT layered clay such as hectorite and laponite.....	2
Figure 2. Difference in microcrystallite arrangement between laponite 'house of cards' structure and hectorite. Laponite tactoids are single TOT layers while a hectorite microcrystallite may contain seven to ten TOT layers.....	3
Figure 3. Surfactant aggregates in the laponite intergallery region.....	5
Figure 4. Synthetic approach to NLO dye inclusion into organically modified laponite.....	5
Figure 5. Head-to-tail hydrogen bonding of J-aggregates.....	6
Figure 6. Structures of various NLO dyes utilized in this experiment.....	9
Figure 7. Relationship between surfactant chain length, asymmetric CH ₂ stretching frequencies (ν_{as}), and gallery height. Hectorite was loaded at 100% of its CEC with surfactant.....	13
Figure 8. Relationship between TMCA packing density in hectorite, asymmetric CH ₂ stretching frequencies (ν_{as}), and gallery height.....	14
Figure 9. XRD spectra of laponite powders and films. OMS films show evidence lamellar ordering.....	16
Figure 10. Schematic representation of two-dimensional ordering. Laponite's 'house of cards' structure is broken up and long range 2-D tiling and superstructure are exhibited in powder XRD.....	16

Figure 11. J-aggregation of DSO3 as a function of surfactant loading level.	
All films were loaded with varied amounts of TMCA and	
1 w/w% DSO3. Films at higher surfactant loading levels phase	
separate causing a decrease in optical transparency.....	19
Figure 12. Extent of J-aggregation as a function of DSO3 loading levels in	
TMCA (50 % of CEC) loaded laponite.....	20
Figure 13. Comparison of UV/VIS spectra of DSR1 included in zinc-laponite	
versus in TMCA (50% CEC) laponite films. Organically modified	
laponite facilitates a higher fraction of J-aggregation than	
unmodified laponite.....	21
Figure 14. UV/Vis spectrum of varied loadings of DSR1 within TMCA	
loaded (50% CEC) laponite.....	22

Introduction

Photonics involves the use of light to acquire, store, process, and transmit information. Nonlinear optical (NLO) materials are crucial for success in the advancement of photonic devices.^{1,2} Success in the advancement of photonic materials relies upon an enhanced understanding of the relationship between material architecture and material properties. Nonlinear optics is the study of the interaction of intense electromagnetic fields with materials to produce modified fields that are different from the input field in amplitude, frequency and phase.³ NLO phenomena are of major importance as they form the basis of optical processing networks, waveguides, photochemical hole burning materials, holographic storage devices, and second harmonic generators.^{4,5}

A new class of photonic materials are inorganic-organic nanocomposites. These hybrid assemblies encompass a wide variety of materials whose inner architectures can be customized for specific optical device applications.^{1,4} Hybrid inorganic-organic materials couple the functionality of organic molecules with the stability of inorganic solids. The inorganic host exhibits the virtues of high surface area, thermal stability, crystallinity, and catalytic capability^{6,7} while the organic guest offers a diverse selection of molecules with electrical, optical, and thermal properties. The synergistic relationship between organic guests and inorganic hosts affords the synthesis of an enormous variety of materials whose properties can be selectively tuned. Rational selection of the two components is indispensable for the fabrication of advanced materials.⁸

Smectite clays exhibit a lamellar structure with important colloidal properties⁹ and present incredibly robust inorganic hosts. These lamellar clays¹⁰ exhibit unique

properties such as templating, two-dimensional ordering, heterogeneous catalysis, and high thermal and temporal stabilities. Laponite and hectorite are examples of such smectite clays that are made up of tetrahedral-octahedral-tetrahedral layers (TOT) (see Figure 1). The octahedral layer is comprised of magnesium cations doped with lithium cations, creating an overall negative charge on the framework. The overall negative charge affords the intercalation of various cations into an intergallery region; these cations bridge the TOT sheets and control lamellar architecture. Intercalated cations can be replaced through a facile cation exchange reaction allowing for the modification of host characteristics such as redox potentials, film stability, electrical, and optical properties.^{11,12}

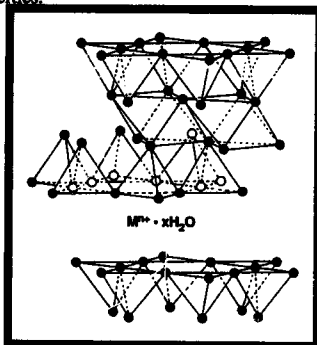


Figure 1. Structure of TOT layered clay such as hectorite and laponite.

Laponite is a synthetic form of hectorite, a naturally occurring clay mineral. Both laponite and hectorite are structurally and chemically similar but differ in layer lattice charge, size of microcrystallites or tactoids, and superstructural arrangements. Laponite tactoids are disk-shaped consisting of a single TOT layer and are

approximately 250 Å in diameter by 10 Å in height. As a result of small tactoid size, laponite has a high charge to surface area ratio and is prone to forming gel-like matrices termed the 'house of cards' structure^{13,14} (see Figure 2). Hectorite has a brick-shaped structure with a much larger tactoid size (10,000 Å x 1000 Å x 100 Å) and consists of approximately seven to ten TOT layers.¹⁵

Three distinct microenvironments result from the cohesion of multiple TOT layers, (a) an intergallery region between adjacent tactoids, (b) the surface of the tactoid, and (c) the microporous spaces between adjacent tactoids. The insertion of cations into the intergallery region (a) is called intercalation. The sizes and hydrophobic characteristics of these microenvironments are affected by charge density, water content, and the extent of clay contact.

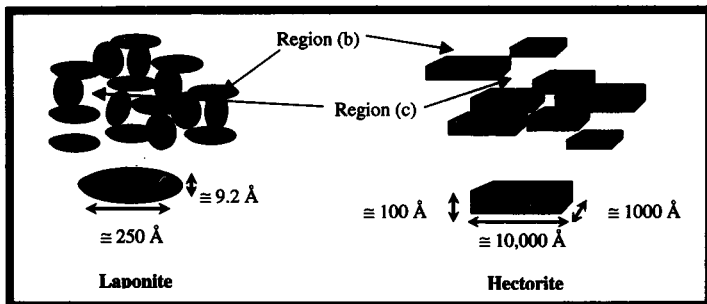


Figure 2. Difference in microcrystallite arrangement between laponite 'house of cards' structure and hectorite. Laponite tactoids are single TOT layers while a hectorite microcrystallite may contain seven to ten TOT layers.

films. Cationic chromophores,^{13,16} surfactants,^{17,18,19} and polymers,^{20,21,22} have all been intercalated into smectite clays previously. Charged nonlinear optical chromophores^{10,23,24,25,26,27} have also been included into smectite clays and have

exhibited great promise. The inclusion of neutral dyes allows for further modification to the hybrid materials and work in this area is unexplored. Phase separations between organic and inorganic components make the synthesis of these materials complicated. The process of initially organically modifying laponite and hectorite using surfactants and subsequently including neutral NLO dyes shows even greater promise for fine control over the hybrid material properties.

The aggregation of surfactant molecules on clay surfaces have been studied extensively.^{28,15,29} Giannelis²⁶ and colleagues have demonstrated that as the packing density and surfactant chain length of surfactants on the clay surface increase the ordering of surfactant chains increases. Four surfactant aggregates result from the extent of surfactant ordering; (a) lateral monolayer, (b) lateral bilayer, (c) paraffin monolayer, and (d) paraffin bilayer (see Figure 3). The extent of surfactant ordering is readily observable with infrared spectroscopy by monitoring asymmetric methylene frequency ($\nu_{as}-CH_2-$) shifts.

Surfactant inclusion provides a driving force for organic nlo dye inclusion in aqueous media by two dimensionally ordering laponite tactoids and rendering the intergallery region organophilic (see Figure 4). The extent of two-dimensional ordering in organically modified laponite as a function of surfactant type and loading density was monitored using powder X-ray diffraction techniques.

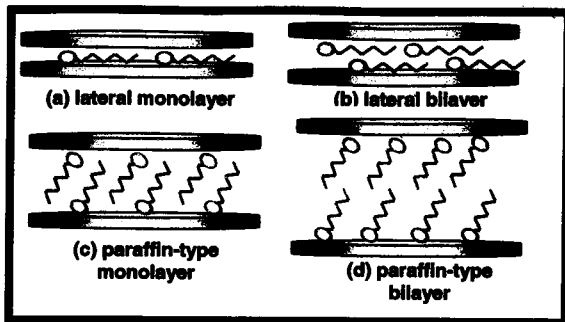


Figure 3. Surfactant aggregates in the laponite intergallery region.

The aggregation of included nonlinear optical chromophores can be monitored through changes in electronic absorption spectra. The type³⁰ and extent of dye aggregation are affected by the nature of dye environment.³¹ These host-guest interactions can be controlled by the choice of functional groups present on the dye molecule. Two types of dye aggregates have been previously revealed, J-type or Scheibe^{19,32,33,34} aggregates and H-type aggregates. Scheibe or J-type aggregation refers to the head-to-tail hydrogen bonding between adjacent dye molecules (see Figure 5).

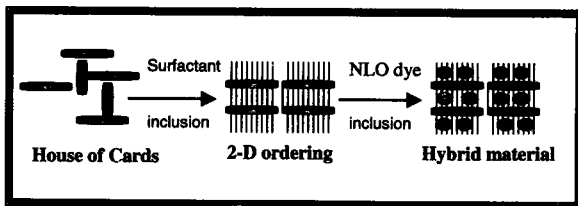


Figure 4. Synthetic approach to NLO dye inclusion into organically modified laponite.

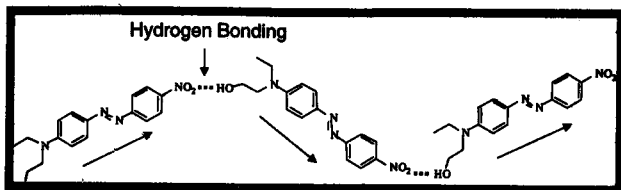


Figure 5. Head-to-tail hydrogen bonding of J-aggregates

J-aggregation is evidenced by a red shift in the absorption spectrum, as well as a new absorbance band associated with dimer or higher aggregate formation. H-type aggregation occurs as a result of π -stacking²⁸ interactions between dye molecules. The absorption spectra of H-aggregates show a characteristic single blue-shifted peak.

The photonic response of nonlinear optical dyes is greatly affected by the type and nature of dye aggregation. J-aggregation leads to a noncentrosymmetric orientation of dipole moments, which has been shown to be requisite for a NLO response, while H-type aggregation causes the cancellation of dipoles and produces no NLO response. The NLO response of these new composite materials can be monitored with the use of Second Harmonic Generation (SHG). SHG occurs when incident light of frequency ω passes through a nonlinear optical medium that then emits the light at twice the input frequency 2ω . SHG characterization can be performed on powders,^{35,36,37} colloidal suspensions,¹² and more recently has been used to probe the noncentrosymmetric arrangement of chromophores within thin films.^{38,39,40,41,42,43,44,45}

In nonlinear optics the induced electric polarization of the nonlinear optical material is a nonlinear function of the strength of the external field. Polarization in intense magnetic fields, such as in a laser, can be described at both the microscopic

(molecular) and macroscopic (bulk) levels. The equation below describes the microscopic interaction with applied electric fields.⁵ Polarization in a nonlinear optical material depends on high order terms of the applied electric field. In the equation below μ_0 is the intrinsic dipole moment of the molecule and F is the electromagnetic field vector. The coefficients α , β , and γ are the polarizability, the hyperpolarizability, and the second hyperpolarizability constants of the molecule. Throughout this work we are only concerned with second hyperpolarizability effects.

$$\mu = \mu_0 + \alpha F + \beta F^2 + \gamma F^3 + \dots$$

The azobenzene and stilbene dyes used in this study exhibit some of the largest β values (125 to $200 \times 10^{-30} \text{ cm}^5/\text{esu}$) commercially available.³ The successful production of materials with high second order nonlinearities is dependent upon two requirements. The first major requirement is the existence of permanent electric dipole moments. Conjugated organic molecules with electron withdrawing-donating moieties^{2, 37, 46, 47, 48, 49, 50, 51, 52, 53} have been shown to be hyperpolarizable in applied electromagnetic fields. The second major requirement for hyperpolarizability is the existence of noncentrosymmetry within the system. The cancellation of dipole moments, such as in π -stacked H-aggregates, produces no NLO effect.

It has been previously demonstrated by Kostuk⁵⁴ that hybrids of neutral NLO dye molecules incorporated into laponite films show evidence of J-aggregation, requisite for SHG. In this work we report on novel hybrids of neutral NLO dye molecules incorporated within organically modified laponite and the selective control over the extent of J-aggregate formation. UV/Vis absorption spectroscopy, X-ray diffraction, and infrared spectroscopy are used to probe the inner architectures of these

hybrid materials and their microenvironments affording a greater understanding of surfactant aggregation on laponite tactoids and the influence of surfactant coated laponite on NLO dye aggregation.

Experimental Methods

Materials. Na⁺-Hectorite with a cation exchange capacity (CEC) of 100 mequiv/100g (Na-Hect), Na_{0.66}[Li_{0.66}Mg_{5.34}Si₈O₂₀(OH)₄]²¹ was obtained from RHEOX, Inc. Na⁺-Laponite RD with a CEC of 72 mequiv/100g (Na-LapRD), Na_{0.7}[Li_{0.3}Mg_{5.5}Si₈O₂₂(OH)₄]⁵⁵ was donated by Southern Clay Products, Inc. The surfactants used in this experiment were tetrabutylammonium (TBA), Triethylhexylammonium (TEHA), trimethyldecyl (TMDA), and trimethylcetylammunium (TMCA) bromide salts. The neutral dyes used for the synthesis of the hybrid materials were disperse red 1 (DSR1) and disperse orange 3 (DSO3). Surfactants and dyes were obtained from Aldrich & Co. and used as received.

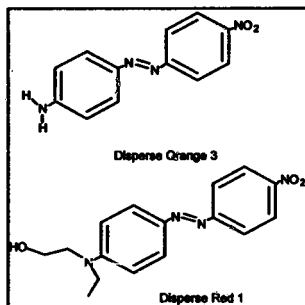


Figure 6. Structures of various NLO dyes utilized in this experiment

Synthesis. Laponite RD is received prepared with sodium as the intergallery cation. The sodium intergallery cation was exchanged with zinc by a cation-exchange reaction between the silicate and excess zinc (twice the exchange capacity of the host). Sodium laponite was monodispersed⁵⁶ by high speed spinning in deionized water for 0.5-1 hour and subsequently loaded with zinc. The zinc/Na-LapRD solution was spun for 24-48 hours allowing for complete exchange. The solution was then centrifuged and washed multiple times with deionized water ensuring the complete removal of sodium cations and counter anions and subsequently re-dispersed in deionized water.

Quaternary alkylammonium halide salts were dissolved in a 50:50 mixture of ethanol and deionized H₂O. The appropriate amount of guest mixture was added to prepared Zn-LapRD in order to attain the desired loading. Loadings are presented as a percentage of the smectite's CEC. The mixture was stirred for 7-12 hours at 50°-70° C. The organically modified silicates (OMS) were subsequently centrifuged and washed extensively with a 50:50 ethanol and deionized water mixture until an AgNO₃ test confirmed the absence of halide anions.

The neutral chromophores were dissolved in acetone and the appropriate wt % of dye was added to either Zn-LapRD or the fabricated OMS. Acetone was removed from the resulting solution using a Buchi rotary evaporator. The mixture was then spun for 24 hrs before being pipetted onto precleaned quartz microscope slides. Glass microscope slides were precleaned with acetone and water. 2 mL of the dye/Zn-LapRD or dye/OMS solution was introduced to the glass substrate and allowed to dry slowly in a humidity-controlled environment, forming an optically transparent thin film.

Characterization. Fourier transform infrared (FTIR) spectroscopy afforded the study of the intercalated surfactant-surfactant interactions and their conformations within the films. FTIR spectra were collected using a Mattson Galaxy 6020 spectrometer with a Spectra Tech Thunderdome ATR attachment allowing for direct characterization of solid films. For each spectrum 128 interferograms were collected and coadded at a nominal resolution of 1 cm^{-1} . Peak frequencies were ascertained using the center of gravity method. Intergallery spacing was monitored using powder X-ray diffraction (XRD). XRD spectra were collected on a Philips PW 1840 diffractometer using 1.788 \AA CoK_α radiation. Electronic absorption spectroscopy was used to study dye-clay interactions. All UV/Vis spectra of films were collected on a HP8453 spectrophotometer. All data were collected under ambient conditions.

Results and Discussion

Organically Modified Silicates. Rational selection of surfactant chain length and loading density is crucial for the creation of an optimal microenvironment for dye inclusion. FTIR spectroscopy coupled with powder XRD affords the probing of the inner architecture of organically modified silicates. Specifically, FTIR studies elucidate the type and nature of surfactant aggregation (Figure 3) and powder XRD monitors the effects of aggregation type on the spacing between tactoid repeat units in the clay films.

Upon cation exchange surfactant molecules enter the intergallery phase space through coulombic attraction to the negative charge residing on the tactoid surface. Surfactant geometry, hydrocarbon chain length, and packing density impact the inner architecture of the smectite clays. As the surfactant chain length was increased FTIR spectra revealed a shift in CH_2 asymmetrical stretching vibrations (ν_{as}) to lower wavenumbers (see Figure 7). The shifting of these bands to lower frequencies indicates that the surfactant chains are adopting a higher trans to gauche ratio, indicative of ordering. As a result of a higher degree of chain ordering an increased intergallery height was observed within hectorite films. An increase in surfactant chain length causes ordering due to an increase in the van der Waals interactions between adjacent surfactant molecules. Chain ordering induces a higher trans/gauche ratio causing the chains to become extended, facilitating an increase in the intergallery spacing height (Figure 2, region (b)). Figure 7 illustrates that TMCA (sixteen carbon chain) undergoes the greatest degree of ordering and causes the greatest increase in gallery height.

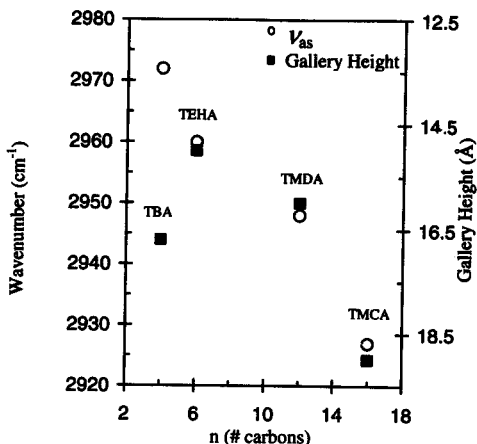


Figure 7. Relationship between surfactant chain length, asymmetric CH₂ stretching frequencies (ν_{as}), and gallery height. Hectorite was loaded at 100% of its CEC with surfactants. TBA is marked in green because it is a spherical molecule with no distinction between head size and chain length. The increase in gallery height with TBA is due to its large spherical head size.

Surfactant packing density also induces surfactant chain ordering and a resultant increased gallery height.

As the amount of surfactant loaded into hectorite increases, the surfactant chains assume a higher trans/gauche ratio and therefore become more ordered, resulting in an increase in intergallery height. Ordering, as the surfactant packing density is increased, is due to an increase in van der Waals interactions between surfactant chains. Figure 8 illustrates the relationship between TMCA surfactant packing density, CH₂ asymmetric stretching frequencies, and gallery height.

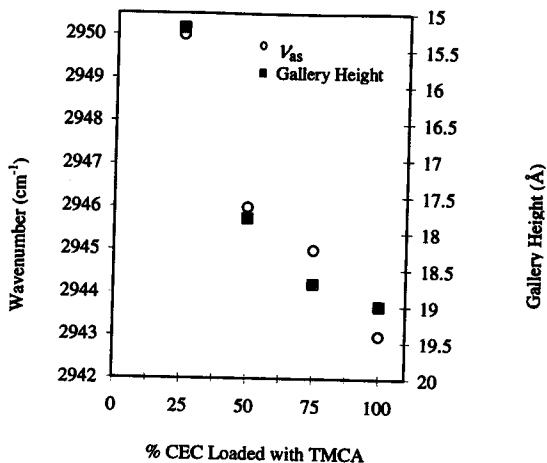


Figure 8. Relationship between TMCA packing density in hectorite, asymmetric CH_2 stretching frequencies (ν_{as}), and gallery height.

Figure 8 also illustrates that control over surfactant loading levels affords fine control over intergallery basal spacing.

Increasing the hydrophobicity of the intergallery region coupled with increasing intergallery spacing provides a driving force for the inclusion of NLO dyes. There is a clear trend between surfactant chain length, surfactant loading, and gallery spacing in hectorite clay films. However this trend does not occur in laponite clay films. We speculate that the lack of this trend in laponite films is due to the formation of the 'house of cards' structure. The formation of laponite's 'house of cards' structure is a result of coulombic interactions between negatively charged faces with positively charged edges. As the surfactant chain length and packing density of

TMCA was increased in laponite films, no increase in gallery height or surfactant chain ordering occurred, however a different yet curious trend was illustrated.

Powder XRD spectra indicate that as surfactant chain length was increased laponite's 'house of cards' structure was broken up by the appearance of two-dimensional tactoid ordering (Figure 9). The intercalation of surfactant into laponite induces a greater level of ordering than in films without surfactant. Ordering results from the coating of laponite tactoids with surfactant. Surfactants inhibit the coulombic attraction between adjacent tactoids and cause a breakdown of the 'house of cards' structure by inhibiting tactoid edge/surface interactions. A high degree of disorder in laponite powder produces an amorphous XRD pattern however a sodium laponite film shows a greater degree of ordering with the growth of a 001 reflection, at a d-spacing of $\sim 12.9 \text{ \AA}$, indicative of lamellar ordering (Figure 10). The introduction of surfactant into the laponite films (TMDA and TEHA OMS films) shows an even greater degree of lamellar ordering as evidenced by: the growth of new peaks associated with the 00 l family of reflections (at d-spacings of approximately 14.4 \AA , 4.7 \AA , and 3.5 \AA) and a sharpening of the 001 reflection.

Furthermore, the presence of a new peak at low angles, with a d-spacing of approximately 44.6 \AA , indicates the presence of superstructure or extended two-dimensional lamellar ordering. The evolution of a low angle peak can be explained with two models (Figure 10). Model 1 proposes the aggregation two adjacent tactoids separated by a surfactant paraffin bilayer while model 2 proposes the aggregation of several adjacent tactoids separated by lateral monolayers.

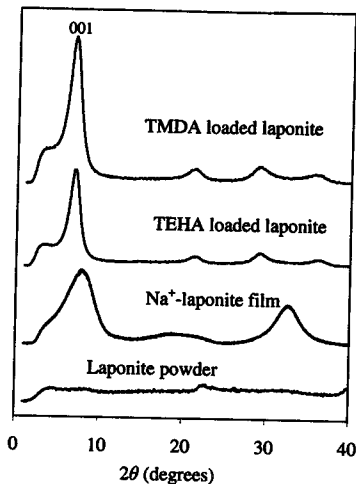


Figure 9. XRD spectra of laponite powders and films. OMS films show evidence lamellar ordering.

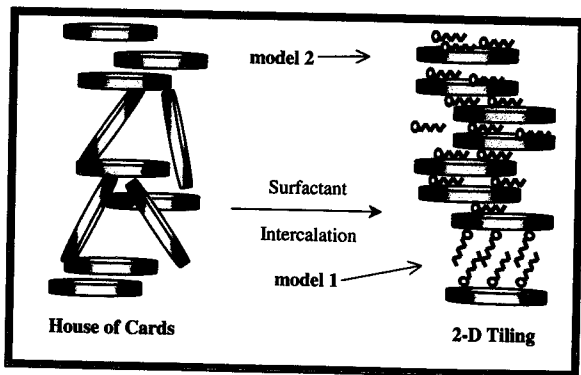


Figure 10. Schematic representation of two-dimensional ordering. Laponite's 'house of cards' structure is broken up and long range 2-D tiling and superstructure are exhibited in powder XRD.

Therefore, organically modifying silicates with the use of surfactants induces two-dimensional lamellar ordering. We speculate that long range two-dimensional ordering is crucial for the enhancement of chromophore J-aggregation. The introduction of surfactant into hectorite affords selective control of both intergallery height and lamellar ordering whilst introduction of surfactant into laponite solely allows for tuning of lamellar ordering. This difference between laponite and hectorite is a function of tactoid size. Fine-tuning of intergallery height does not occur in surfactant loaded laponite films due to the presence of a mixture of surfactant aggregates (see Figure 10). Although surfactants do not afford the same control over laponite's intergallery size as they do with hectorite, due to difference in tactoid size, laponite serves as a superior material for photonic applications. Hectorite composites are optically opaque in the visible region while laponite is transparent lending itself to photonic applications. Hectorite's large tactoid size scatters light whereas laponite's small tactoid size does not.

Although high loading levels of surfactant into laponite facilitate the greatest degree of ordering, several problems arise. High surfactant loadings induce the highest degree of hydrophobicity of tactoids and cause tactoid flocculation in aqueous media, causing poor film quality. For example, laponite films loaded with TMCA at 100% of the CEC exhibit heterogeneity and cracking due to tactoid flocculation. In fact, surfactant loadings greater than 50% of the CEC produce poor quality films. Therefore, films prepared for NLO dye introduction should not exceed surfactant loadings of 50% of the CEC. Surfactant loadings at this level are optimal as they

maintain high film quality and optical transparency while rendering laponite tactoids hydrophobic thus promoting dye inclusion.

NLO dye inclusion into Organically Modified Laponite. Organically modified laponite provides an improved host system for the introduction of nonlinear optical chromophores. Two distinct nlo dyes, DSR1 and DSO3, were introduced into TMCA loaded (50% CEC) laponite films. Both DSR1 and DSO3 are diazobenzene-based dyes differing solely in their terminal moieties (see Figure 6). Previous studies⁵⁴ illustrated that the dye loading levels have not exceeded 10 wt %. We speculate that higher loadings as well as higher fractions of J-aggregation will yield an enhanced NLO response. J-aggregation was monitored with UV/VIS and FTIR spectroscopies. Because DSO3 contains a terminal amine group (see Figure 6), hydrogen-bonding interactions can be easily monitored with FTIR.

Inclusion of DSO3. Surfactant loading levels play a critical role with respect to the fraction of J-aggregated species in the DSO3 system. As the surfactant loading levels were increased, J-aggregation was turned off, providing a means of selectively tuning NLO activity. In fact, the decrease in the red shifted J-aggregated band was so dramatic that it was observed visually (Figure 11). Films at lower surfactant loading levels were much redder in color than those at higher surfactant loadings, which were orange, matching the color of the bulk dye. Visual evidence was confirmed by monitoring the J-aggregation of DSO3 with FTIR. Bulk dye terminal N-H bands appeared at 3399 and 3499 cm^{-1} and were shifted and broadened to 3240 and 3397 cm^{-1} , respectively, within TMCA-laponite films. Shifting to lower frequencies accompanied by broadening is characteristic of hydrogen bonding and indicates the J-

aggregation of DSO3. As surfactant packing density increases on laponite's surface the interaction between the dye and clay is minimized, turning off J-aggregation. The deactivation of J-aggregation at high surfactant loading levels confirms that an interface between the chromophores and laponite is crucial for J-aggregation.⁵⁴

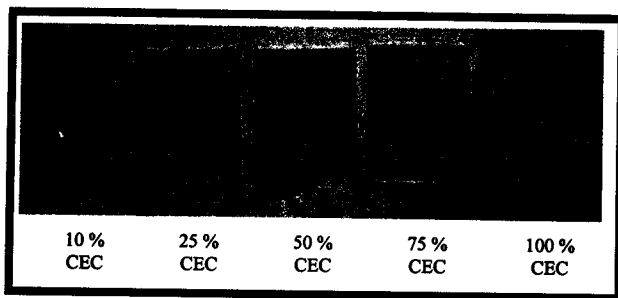


Figure 11. J-aggregation of DSO3 as a function of surfactant loading level. All films were loaded with varied amounts of TMCA and 1 w/w% DSO3. Films at higher surfactant loading levels phase separate causing a decrease in optical transparency.

TMCA loadings above 50% of the CEC turn the J-aggregation of DSO3 as well as forming poor quality films due to phase separation in aqueous media. Therefore, TMCA loadings of 50% of the CEC were determined to offer a compromise between turning J-aggregation off and rendering laponite organophilic so as to provide a driving force for the inclusion of higher loadings of DSO3 in water.

DSO3 w/w% loadings were varied within organically modified laponite in order to study the effect of the surfactant on J-aggregation (Figure 12). The fraction of J-aggregated species reached a maximum at 1 w/w% DSO3 in TMCA exchanged (50% CEC) laponite. In unmodified zinc-laponite films loaded with DSO3 the fraction of J-aggregated species also reached a maximum at 1 w/w%, however at

DSO3 loadings above 5 w/w% the absorption band blue shifted back to the bulk dye peak (490 nm). In organically modified films, higher DSO3 loadings maintained a fraction of J-aggregated species. This higher fraction is significant as it may lead to observable nlo response.

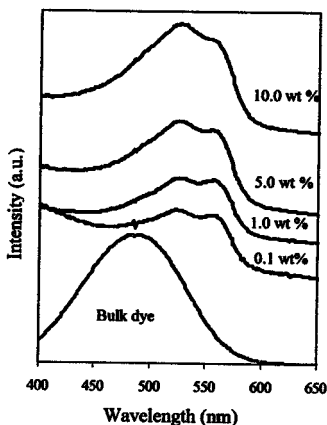


Figure 12. Extent of J-aggregation as a function of DSO3 loading levels in TMCA (50% of CEC) loaded laponite.

Inclusion of DSR1. DSR1 exhibited very different behavior from DSO3 within organically modified laponite. Surfactant loadings increase the degree of red shifting attributed to the J-aggregation of DSR1.²⁸ A comparison of films containing 5 w/w% DSR1 included in zinc-laponite versus in TMCA (50% CEC) laponite films illustrates further red shifting to longer wavelengths (Figure 13). It has been shown that the exclusion of water in films increases the J-aggregation.⁵⁴ We speculate that rendering

laponite organophilic excludes water from the intergallery phase space thus increasing J-aggregation.

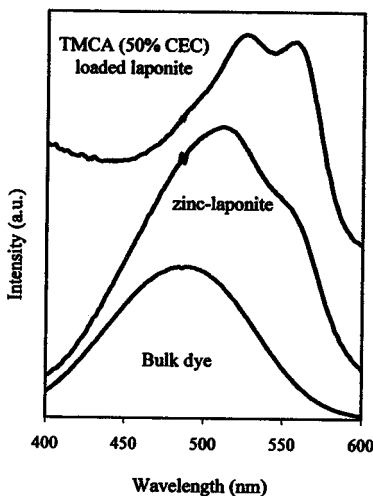


Figure 13. Comparison of UV/VIS spectra of DSR1 included in zinc-laponite versus in TMCA (50% CEC) laponite films.

Not only does organically modified laponite induce a higher fraction of J-aggregated DSR1 but the presence of surfactant also increases the maximum loading level of no chromophores. It has previously been thought that DSR1 loading above 5 w/w% would lose their J-aggregated configuration. Cases in which zinc-laponite was loaded with greater than 5 w/w% DSR1 formed poor quality films due to flocculation of DSR1 molecules coupled with phase separation.⁵⁴ TMCA loaded laponite (50%

CEC) permits the inclusion of much higher loadings of DSR1 without the loss of film quality (Figure 14).

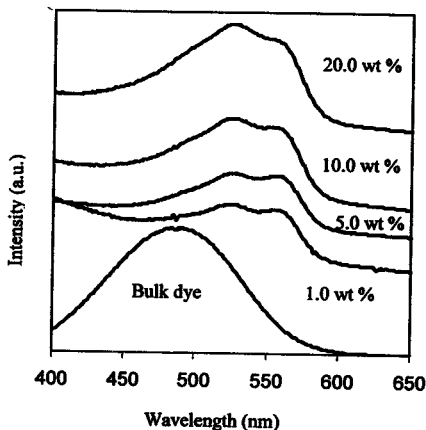


Figure 14. UV/VIS spectra of varied loadings of DSR1 within TMCA loaded (50% CEC) laponite.

The increase in J-aggregated species and increase in maximum dye loadings can be attributed to an increase in the two dimensional ordering of laponite tactoids by the intercalation of organic surfactants. Two-dimensional ordering of tactoids increases the effective surface area available for interaction with DSR1. Unlike DSO3, DSR1 did not blue shift as surfactant loading was increased. This difference in behavior can be attributed to the structure of the dye molecules (see Figure 6). DSO3 contains an amine functional group at its terminus whereas DSR1 contains hydrocarbon moieties. The presence of hydrocarbons on DSR1's terminus may enhance hydrogen-bonding interactions between chromophores due to their increased

solubility in the organic intergallery phase space. Rendering the intergallery region organophilic also decreases the chance of phase separation affording quality films with increased dye loadings.

Conclusions

Organically modifying laponite tactoids through the use of surfactants affords selective control over nonlinear optical chromophores aggregation. Rational selection of surfactant and NLO chromophore type lends to enhanced photonic materials. Longer alkylammonium surfactant chains and higher packing densities assist in breaking up laponite's 'house of cards' architecture inducing two-dimensional ordering of tactoids. Two-dimensional ordering coupled with an increase in the hydrophobicity of the intergallery region provides the necessary environment for NLO chromophore inclusion.

NLO effects should be enhanced with an increase in the J-aggregation of chromophore molecules, resulting from the noncentrosymmetric alignment of molecular dipole moments. DSO3 forms J-aggregates in zinc-laponite films, however dye loadings above 1 w/w% result in a decrease in J-aggregation, exemplified by a blue shift in the absorption band. TMCA loaded laponite provided a means for maintaining J-aggregation in DSO3 loadings up to 10 w/w%, ten times greater than previously reported.⁵⁴ The extent of DSO3 chromophore J-aggregation was selectively tuned by varying surfactant loading levels. Greater surfactant loadings deactivated DSO3 J-aggregation. We found that laponite loaded at 50% of the CEC with TMCA optimized DSO3 J-aggregation while maintaining film quality and providing the necessary hydrophobic environment conducive to increasing dye loading levels.

Organically modifying laponite also enhances the material properties of DSR1 loaded films. Rendering the intergallery region hydrophobic and two-dimensional ordering shows a marked effect on DSR1 J-aggregation. Most significantly, the presence of surfactant in the intergallery phase space increases J-aggregation through the exclusion of water within the intergallery region. In addition, the maximum dye loading level was increased to 20 w/w%, while maintaining the improved J-aggregation.

Future Work

Organically modified laponite has been shown to increase the fraction of J-aggregation of DSR1 as well as make it feasible to include higher loadings of DSR1 and DSO3. However, further studies should be performed in order to gain a more fundamental understanding of these effects on dye aggregation. Dye/surfactant interactions within laponite frameworks have not been previously reported. One route for the elucidation of these interactions may come through the intercalation of fluorescent surfactants.⁵⁷ Monitoring the fluorescence of surfactants as NLO dyes are included into films may reveal dye/surfactant interactions. Surfactant intercalation yields are not yet accurately known. For example, exchanging surfactant at 50% of the cation exchange capacity may yield lower exchanges. Thermogravimetric analysis may provide more detailed information on surfactant intercalation yields. Thus far all hybrid films have been fabricated on glass microscope slides. The exploration of various other substrates, such as silicon metal, would be advantageous for device implementation. Finally, SHG studies must be performed on these hybrid materials.

References

- ¹ Bennion, I. *Inst. Phys. Conf. Ser. No 103: Introduction*, 1989.
- ² Marder, S.R.; Perry, J.W. *Adv. Mater.* 1993, 5(11), 804-815.
- ³ Saleh, B.E.A.; Teich, M.C. *Fundamentals of Photonics*; John Wiley & Sons: New York, 1991.
- ⁴ Seto, J.; Tamura, S.; Asai, N.; Kishii, N.; Kijina, Y.; Matsuzawa, N. *Pure and Appl. Chem.* 1996, 68(7), 1429-1434.
- ⁵ Hecht, J. *The Laser Guidebook*; McGraw-Hill: New York, 1986.
- ⁶ Mallouk, T.E.; Gavin, J.A. *Acc. Chem. Res.* 1998, 31, 209-217.
- ⁷ Ogawa, M.; Kuroda, K. *Chem.Rev.* 1995, 95, 399-438.
- ⁸ Salvador, P.A.; Mason, T.O.; Hagerman, M.E.; Poeppelmeier, K.R. Layered Transition Metal Oxides and Chalcogenides. In *Chemistry of Advanced Materials: An Overview*. L. V. Interrante, L.V., Hampden-Smith, M.J. Eds.; Wiley-VCH Publishers: New York, 1998; 449-498.
- ⁹ Van Olphen, H. *An Introduction to Clay Colloid Chemistry*; John Wiley & Sons: New York, 1977.
- ¹⁰ Alonso, P.J.; Fraile, J.M.; Garcia, J.; Garcia, J.I.; Martinez, J.I.; Mayoral, J.A.; Sanchez, M.C. *Langmuir* 2000, 16, 5607-5612.
- ¹¹ Coradin, T.; Clément, R. *Chem Mater.* 1996, 8, 2153-2158.
- ¹² Mourchid, A.; Delville, A.; Lambard, J.; Lécolier, E.; Levitz, P. *Langmuir* 1995, 11, 1942-1950.
- ¹³ Yan, E.C.Y.; Eisenthal, K.B. *J. Phys. Chem. B* 1999, 103, 6056-6060.
- ¹⁴ López Arebeloa, F.; Herrán Martínez, J.M.; López Arebeloa, T.; López Arebeloa, I. *Langmuir* 1998, 14, 4566-4573.

- ¹⁵ Annabi-Bergaya, F.; Estrade-Swarckopf, H.; Van Damme, H. *J. Phys. Chem.* **1996**, 4120-4126.
- ¹⁶ Chernia, Z.; Gill, D. *Langmuir* **1999**, 15, 1625-1633.
- ¹⁷ Esumi, K.; Takeda, Y.; Goino, M.; Ishiduki, K.; Koide, Y. *Langmuir* **1997**, 13(9), 2585-2587.
- ¹⁸ Nakamura, T.; Thomas, J.K. *J. Phys. Chem.* **1986**, 90, 641-644.
- ¹⁹ Vaia, R.A.; Teukolsky, R.K.; Giannelis, E.P. *Chem. Mater.* **1994**, 6, 1017-1022.
- ²⁰ Liang, L.; Liu, J.; Gong, X. *Langmuir* **2000**, 16, 9595-9899.
- ²¹ Eastman, M.P.; Bain, E.; Proter, T.L.; Manygoats, K.; Whitehorse, R.; Parnell, R.A.; Hagerman, M.E. *Appl. Clay Sci.* **1999**, 15, 173-185.
- ²² Hengzhen, S.; Lan, T.; Pinnavaia, T.J.; *Chem. Mater.* **1996**, 8, 1584-1587.
- ²³ Sonobe, K.; Kikute, K.; Takagi, K. *Chem. Mater.* **1999**, 11, 1089-1093.
- ²⁴ Gessner, F.; Schmitt, C.C.; Neumann, M.G. *Langmuir* **1994**, 10, 3749-3753.
- ²⁵ Coradin, T.; Nakatani, K.; Ledoux, I.; Zyss, J.; Clément, R. *J. Mater. Chem.* **1997**, 7(6), 853-854.
- ²⁶ Chaudhuri, R.; López Arebeloa, F.; López Arebeloa, I. *Langmuir* **2000**, 16, 1285-1291.
- ²⁷ Ogawa, M. *Chem. Mater.* **1996**, 8(7), 1347-1349.
- ²⁸ Vaia, R.A.; Teukolsky, R.K.; Giannelis, E.P. *Chem. Mater.* **1994**, 263, 658-660.
- ²⁹ Umemura, Y.; Yamagishi, A.; Schoonheydt, R.; Persoons, A.; Schryver, F. *Langmuir* **2001**, 17, 449-455.
- ³⁰ Brahim, B.; Labbe, P.; Reverdy, G. *Langmuir* **1992**, 8, 1908-1919.
- ³¹ Liu, X.; Thomas, J.K. *Langmuir* **1991**, 7, 2808-2816.
- ³² Möbius, D. *Adv. Mater.* **1991**, 7, No. 5, 437-444.
- ³³ Von Berlepsch, H.; Böttcher, C.; Dähne, L. *J. Phys. Chem. B* **2000**, 104, 8792-8799.
- ³⁴ Friedrich, J.; Schneider, S. *Adv. Mater.* **1996**, 7(5), 435-436.

- ³⁵ Kurtz, S.K.; Perry, T.T. *J. Appl. Phys.* **1968**, *39*(8), 3798-3813.
- ³⁶ Dougherty, J.P.; Kurtz, S.K. *J. Appl. Cryst.* **1976**, *9*, 145-158.
- ³⁷ Kiguchi, M.; Kato, M.; Kumegawa, N.; Taniguchi, Y. *J. Appl. Phys.* **1994**, *75*(9), 4332-4339.
- ³⁸ Kim, H. K.; Kang, S.; Choi, S.; Min, Y.; Yoon, C. *Chem. Mater.* **1999**, *11*, 779-788.
- ³⁹ Li, F.; Jin, L.; Huang, C.; Zheng, J.; Gui, J.; Zhao, X.; Liu, T. *Chem Mater.* **2001**, *13*, 192-196.
- ⁴⁰ Shimazaki, Y.; Ito, S. *Langmuir* **2000**, *16*, 9478-9482.
- ⁴¹ Liu, Y.; Hu, W.; Xu, Y.; Liu, S.; Zhu, D. *J. Phys. Chem. B* **2000**, *104*, 11859-11863.
- ⁴² Yam, V.W.; Yang, Y.; Yang, H.; Cheung, K. *Organometallics* **1999**, *18*, 5252-5258.
- ⁴³ Ashwell, G.J.; Walker, T.W.; Leeson, P. *Langmuir* **1998**, *14*, 1525-1527.
- ⁴⁴ Koetsch, M.; Lashewsky, A.; Mayer, B.; Rolland, O.; Wisserhoff, E. *Macromolecules* **1998**, *31*, 9316-9327.
- ⁴⁵ Yam, V.; Wang, K.; Wang, C.; Yang, Y.; Cheung, K. *Organometallics* **1998**, *17*, 2440-2446.
- ⁴⁶ Prasad, P.N.; Reinhardt, B.A. *Chem. Mater.* **1990**, *2*, 660-669.
- ⁴⁷ Meyers, F.; Brédas, J.L. *International Journal of Quantum Chemistry* **1992**, *42*, 1595-1614.
- ⁴⁸ Kaino, T.; Tomaru, S. *Adv. Mater.* **1993**, *5*(3), 172-178.
- ⁴⁹ Marder, S.R.; Sohn, J.E.; Stucky, G.D. *ACS Symposium Series* **455**, **1991**.
- ⁵⁰ Groenedaal, L.; Bruining, M.J.; Hendrick, E.H.J.; Persoons, A.; Vekemans, J.A.J.M.; Havinga, E.E.; Meijer, E.W. *Chem. Mater.* **1998**, *10*, 226-234.
- ⁵¹ Dalton, L.R.; Harper, A.W.; Ghosn, R.; Steier, W.H.; Ziari, M.; Fetterman, H.; Shi, Y.; Mustachich, R.V.; Jen, A.K.Y.; Shea, K.J. *Chem. Mater.* **1995**, *7*, 1060-1081.
- ⁵² Marder, S.R.; Perry, J.W.; Yakymyshyn, C.P. *Chem. Mater.* **1994**, *6*, 1137-1147.

- ⁵³ de la Torre, G.; Vázquez, P.; Aguiló-López, F.; Torres, T. *J. Mater. Chem.* **1998**, *8*(8), 1671-1683.
- ⁵⁴ Kostuk, M. "Self-assembled aggregates of neutral nlo dyes in smectite clay films." Senior thesis with M.E. Hagerman. Union College, 2001.
- ⁵⁵ Saunders, J.M.; Goodwin, J.W.; Richardson, R.M.; Vincent, B. *J. Phys. Chem. B* **1999**, *103*, 9211-9218.
- ⁵⁶ Laponite Technical Directory, Laporte, Inc. (<http://www.laponite.com>)
- ⁵⁷ Nakamura, T.; Thomas, J.K. *J. Phys. Chem.* **1986**, *90*, 641-644.